Dalton Transactions

Accepted Manuscript

ROYAL SOCIETY OF CHEMISTRY

www.rsc.org/dalton

A study on the formation of the nitro radical anion by ornidazole and its significant decrease in a structurally characterized binuclear $Cu^{(II)}$-complex: impact in biology

Ramesh Chandra Santra[a], Durba Ganguly[a], Jyotsna Singh[b], Kasturi Mukhopadhyay[b], *Saurabh Das[a]

Department of Chemistry (Inorganic Section), Jadavpur University, Kolkata – 700 032, I N D I A.

School of Environmental Sciences, Jawaharlal Nehru University, New Delhi – 110 067, I N D I A.

***Corresponding author. Tel : +91 8902087756; Fax: +91 33 24146223**

E-mail address : sdas@chemistry.jdvu.ac.in; dasrsv@yahoo.in

Abstract

An acetate bridged binuclear $Cu^{(II)}$ complex of the antiparasitic drug ornidazole was synthesized and characterized by different techniques. Structure of the complex determined by single crystal X-ray diffraction was found to be paddle wheel. Enzyme assay experiments performed under anaerobic conditions on ornidazole and its $Cu^{(II)}$-complex using xanthine oxidase as a model nitro-reductase suggests complex formation is able to cause a significant decrease in the reduction of the nitro group on the imidazole ring. Although not directly coordinated to the metal center, such decrease in generation of nitro radical anion through complex formation is important for its reported neurotoxicity. Decrease in nitro radical anion also implies the complex could be less cytotoxic since reduction products of 5-nitroimidazoles interact with DNA causing destruction in double helical structure and strands leading to inhibition of protein synthesis. This could be a disadvantage from the standpoint of drug efficacy. For this reason, other aspects associated with drug action of 5-nitroimidazoles, like binding to DNA, were studied. Experiments using cyclic voltammetry revealed binding of the complex was almost comparable to ornidazole. Bactericidal activity of ornidazole and the complex was studied on two separate bacterial strains showing the complex was comparable to ornidazole. Since generation of nitro radical anion is known to affect the central nervous system adversely, this study showing its controlled formation by the complex is important. The study showed an ability of the complex to decrease the generation of $NO_2^{\bullet -}$ to an extent that struck the correct balance for beneficial activity since cytotoxicity due to ornidazole was not affected.

Keywords

Ornidazole, crystal structure, xanthine oxidase, nitro-radical anion, DNA binding, cyclic voltammetry, antibacterial activity.

Introduction

5-nitroimidazoles are heterocyclic compounds with proven efficacy on a number of parasitic and bacterial infections.[1-3] Being small molecules they efficiently enter parasites or infecting bacteria [4]. Metronidazole (Mnz), tinidazole (Tnz) and ornidazole (Onz) are important members of the 5-nitroimidazole family having recognized efficacy. The molecules themselves are not active but anaerobic reduction forms the cytotoxic nitro radical anion responsible for its efficacy.[1-4] These compounds are reduced in the hydrogenosome of the parasite by enzymes like pyruvate ferredoxin oxidoreductase (PFOR) where they act as electron sink, capturing electrons from reduced ferredoxin that would otherwise have been donated to hydrogen ions to form hydrogen gas in a hydrogenase reaction.[5,6] Since parasites lack mitochondria they use hydrogenosomes to accomplish fermentative carbohydrate metabolism with hydrogen as the electron acceptor.[5] Reduction of the nitro group in 5-nitroimidazoles is important for it helps these drugs to enter the cell by passive diffusion.[4,6] Reduction is reported to equip them, enabling more drugs to enter the cell by creating a favorable concentration gradient while reduction proceeds intra-cellularly.[4-6] Once inside the cell, the nitro radical anion binds to DNA, disrupting or breaking strands and is a cause of cell death.[6,7]

Although an extremely important class of drugs for different types of infections several problems confront 5-nitroimidazoles. The two main areas of concern are that of drug resistance and neuro-toxic side effects.[8-13] Clinical resistance exists if there is a failure to cure an infection even after at least two consecutive courses of the drugs.[4] Although accurate figures are not available, an estimate suggests ~ 2.5-5.0 % of all cases of trichomoniasis for example, display some level of resistance to Mnz.[5,13] Resistance affects both aerobic and anaerobic mechanisms. In resistance by aerobic mechanisms, there is a decrease in transcription of the ferredoxin gene, decreasing the

ability of the cell to activate 5-nitroimidazoles. Reduced ferredoxin expression results in lowered activation for which there are fewer drugs inside the cell. Besides, oxygen-scavenging pathways are affected. In anaerobic resistance, the performance of PFOR and hydrogenase are decreased or rendered non-existent. Decreased hydrogenase activity, together with reduction in hydrogen production becomes a crucial factor in impaired oxygen-scavenging mechanisms in the hydrogenosome. Since oxygen is an efficient electron receptor, increased levels of cellular (hydrogenosomal) oxygen result in impaired reduction and activation of 5-nitroimidazoles. Therefore, when these drugs are not reduced, concentration becomes similar in intracellular and extracellular fluids and no additional drug enters the cell. Moreover, in the presence of oxygen, reduced nitro free radical is oxidized to its native form with simultaneous formation of superoxide anion achieving only limited cell damage (by superoxide anions) compared to cell death by nitro free radicals.[1]

Owing to aspects of drug resistance reported for Mnz and Tnz, Onz [1-chloro-3-(2-methyl-5-nitro-1*H*-imidazol-1-yl)propan-2-ol], another 5-nitroimidazole, is currently being tried in different pharmaceutical formulations. Although formation of nitro radical anion is important for drug efficacy, too much formation is harmful, being a reason for concern. Hence suitably modified forms that generate the correct amount necessary for cytotoxic action and leave no excess could take care of toxic side effects. To look at such alternatives we prepared a Cu(II) complex of Onz.

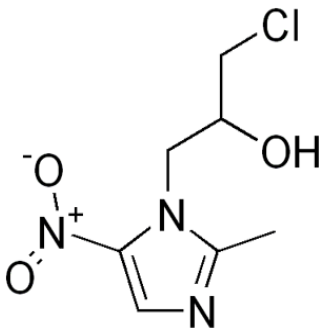

Structure of ornidazole (Onz)

Results and discussion

Structure description of $[Cu_2(OAc)_4(Onz)_2]$

The compound crystallizes in monoclinic space group $P2_1/c$. Structure determination reveals it is a discrete, centrosymmetric dimeric complex, where two different acetate units connect two copper(II) centers to form a paddle-wheel $Cu_2(CO_2)_4$ dinuclear secondary building unit, in which each copper(II) centre is connected to Onz. ORTEP3 view of $[Cu_2(OAc)_4(Onz)_2]$ with 30% ellipsoid probability is shown in Figure 1. In the dimer, two square-pyramidal copper(II) centers are bridged by two centrosymmetrically related acetate anions in μ-1,3 fashion leading to relatively small Cu…Cu distance [2.648(5) Å]. Within the dimeric unit, each of the two square-pyramidal copper(II) centers is coordinated equatorially by four oxygen atoms (O1, O2, O3 and O4) of acetates, comprising the basal plane [bond length lying between 1.948(1) Å and 1.981(1) Å]. One nitrogen atom, N(1), from an Onz ligand coordinates axially at a rather long distance (2.185(3) Å) furnishing a square-pyramidal (4+1) geometry for each copper(II) center in the dimeric complex. A summary of the crystallographic data is provided in Table 1. Selected bond lengths and bond angles are given in supplementary information (Tables ST1 and ST2 respectively). The geometry of a penta-coordinated metal complex may conveniently be measured by the Addison parameter[14], (trigonality index, $\tau = (\alpha-\beta)/60$, where α and β are the two largest L–M–L angles of the coordination sphere) that is ideally zero for a square-pyramidal complex and is one for a trigonal bi-pyramidal one. In the present case, copper(II) centres assume square pyramidal geometries with Addison parameter 0.01. As usual for square pyramid

structures, the copper(II) centres are slightly pulled out of the mean square planes towards the apical donor atoms at distances of 0.2095(4) Å.

The hydroxyl H atoms (H6) attached to O7, forms bifurcated intermolecular H bond with the nitrogen atom N3 and oxygen atom O5 [Figure S1]. Details of the H-bonding are given in Supplementary Information (Table ST 3).

Spectroscopic studies

UV-VIS spectra

Electronic spectra for Onz and the complex show intense UV bands at 318 nm attributed to intra-ligand (IL) transitions. The band at 704 nm for the complex could be assigned to the characteristic d-d transition [dxy, dyz $\rightarrow$ $d_x2_{-y}2$] for $Cu^{(II)}$. However, as expected intensity of the peak at 704 nm was very weak [ε = 72 $M^{-1}cm^{-1}$]. Electronic spectra of the complex (in solution) recorded at different time intervals within a span of 24 hours showed no significant change indicating it was stable with no dissociation of any kind. The value of ε at 318 nm was 8082 $M^{-1}cm^{-1}$ for ornidazole and 17990 $M^{-1}cm^{-1}$ for $[Cu_2(OAc)_4(Onz)_2]$.

IR spectra

IR spectrum of Onz shows a band at 1538.21 cm^{-1} assigned to $\nu_{(C=N)}$ imidazole ring stretching that shifts to higher wavenumbers 1551 cm^{-1} in case of the complex suggesting coordination of the metal ion by imidazole nitrogen (Fig. S2 and S3). The two NO_2 stretching vibrations, ν_{as} 1471 cm^{-1} and ν_s 1385.92 cm^{-1} in the complex were similar to Onz clearly indicating NO_2 does not participate in bonding. IR spectrum of the complex (Fig. S3) shows two intense bands at 1630 cm^{-1} and 1425 cm^{-1} respectively that were absent in Onz being characteristic of ν_{as} (CO_2) and ν_s (CO_2). The magnitude of splitting $\Delta\nu$ (CO_2) being 205 cm^{-1} that is generally observed for

bridging acetates indicating presence of such units in the complex. X-ray crystal structure and IR data corroborate each other and was in agreement with similar structures reported earlier.[15-17]

Magnetic property

The effective magnetic moment recorded for the complex at 299 K (1.23 BM) was significantly lower than that expected for d^9 configuration suggesting reasonably strong anti-ferromagnetic coupling between $Cu^{(II)}$ centers. The value was close to μ_{eff} values reported for $Cu^{(II)}$ acetates and other binuclear $Cu^{(II)}$ compounds, supporting a dimeric structure with interaction between $Cu^{(II)}$ centres. While discussing the X-ray crystallographic data we mentioned that in each binuclear unit, $Cu^{(II)}$ centers were found separated by 2.648 Å representing moderately strong $Cu^{(II)}$….$Cu^{(II)}$ interaction. The magnetic susceptibility measurements only strengthened this thought further.

EPR spectrum

The EPR spectrum at X-band frequency for $[Cu_2(OAc)_4(Onz)_2]$ taken from 0 to 800 mT at 25 °C showed three signals at 30 mT (Hz_1), 470 mT ($H\perp_2$), and 605 mT (Hz_2) respectively (Fig. S4). Small resonance signals in the region from 300 – 400 mT were due to monomer impurities which are often observed for carboxylato-bridged $Cu^{(II)}$ compounds.[18,19] The spin Hamiltonian for the triplet state of dimeric copper (II) compounds may be represented by Eq. 2,

$$H = \beta\, HgS + DSz^2 + E(Sx^2 - Sy^2) - 2/3D \qquad (2)$$

where D and E are zero-field splitting parameters, β is the Bohr magneton, and x, y, and z are principal axes coordinate system fixed with respect to the Cu–Cu bond[20]. Since in case of a powdered sample it is impossible to align the magnetic field along a given direction, the observed spectrum is the sum over all possible orientations. Three resonance fields observed for such axially symmetric complexes and the g values (g|| and g⊥) at room temperature for a powdered sample are related by the following equations:

$$H\perp_2 = (g_e/g\perp)^2[H_0(H_0+D')]$$

$$Hz_1 = - (g_e/g_z) (H_0-D')$$

$$Hz_2 = (g_e/g_z) (H_0+D')$$

where $H_0 = h\nu/g_e\beta$ and $D' = D/g_e\beta$. The g values obtained using the above equations, 2.35 (g||) and 2.04 (g⊥) compare well with those found for a large number of dimeric $Cu^{(II)}$-carboxylato complexes possessing axial symmetry.[18–23] The EPR data was characteristic of tetragonal structures ($g_\parallel > g\perp$) where the unpaired electron was present in a $d_{x^2-y^2}$ orbital.

Enzyme assay

In the presence of the enzyme xanthine oxidase (XOD), hypoxanthine is reported to reduce nitro-imidazoles to a nitro radical anion.[24] This reduction was followed by monitoring the loss of absorbance of Onz, the complex and a 1:1 mixture of Onz and Cu(II) taken as $Cu(OAc)_2.H_2O$ without pre-complexation at 320 nm for a specified period of time.[24] Enzyme assay revealed there was a decrease in absorbance for Onz but not for the complex. In case of the mixture the decrease in absorbance at 320 nm was less than Onz but greater than the complex. Fig. 2(A) and Fig. 2(B) indicate unlike Onz, $[Cu_2(OAc)_4(Onz)_2]$ did not show a gradual decrease in absorbance. While the nitro group in free Onz was reduced, the same in case of the complex as well as the 1:1 mixture of Cu(II) and Onz was affected, registering comparatively insignificant decrease at 320 nm (Fig. 3). This was inspite the fact that the complex possesses two nitro groups in its structure. The change in absorbance at 320 nm for the 1:1 mixture of Onz and $Cu(OAc)_2.H_2O$ is shown in Fig. 2(C). Thus the metal ion ($Cu^{(II)}$) is involved in some way in preventing the reduction of the nitro group. This could happen due to two reasons. One could be that the orientation of the nitro group in the complex was not quite favorable for reduction i.e.

the directional covalent bonds of the -NO_2 moiety was not properly oriented to accept electrons from hypoxanthine. The other possibility is reduction of -NO_2 to nitro radical anion was followed by an intramolecular electron transfer to the $Cu^{(II)}$ centre thus regenerating -NO_2.[25-27] In either case, the absorbance at 320 nm would remain more or less constant which was actually observed. Whatever little decrease was observed for absorbance of the complex at 320 nm was attributed to either a partial reduction of the nitro centre or inability of all nitro-radical anions formed to transfer their electron to $Cu^{(II)}$. In case of the 1:1 mixture of Onz and Cu(II), upon mixing they may undergo chemical reaction to some extent to form the complex. Therefore, the decrease in reduction of the nitro radical anion in case of the mixture with respect to Onz may be attributed to a combination of *in situ* complex formation as well as the presence of free Cu(II) in the medium. In case of the complex, this has a lot of significance since it is largely believed reduction products of 5-nitroimidazoles interact with DNA causing destruction of double helical structure leading to inhibition of protein synthesis and cell death, a reason for its efficacy on target systems (parasites and bacteria). The same nitro radical anion is toxic to the central nervous system. Hence, any attribute that can modulate the formation of the nitro-radical anion should be able to reduce toxic side effects. In order to see if the Cu(II) complex of Onz was effective as Onz itself we performed a study of Onz and its Cu(II) complex on two different bacterial strains and the results are discussed later.

Cyclic voltammetric studies

The cyclic voltammogram of Onz in aqueous buffer at a scan rate of 0.1 V s^{-1} shows a reduction peak at − 900 mV against Ag/AgCl, satd. KCl. [Figure S5]. The peak was assigned to reduction of –NO_2 on the imidazole ring of Onz.[28-31] Cyclic voltammogram of a similar concentration of $[Cu_2(OAc)_4(Onz)_2]$ showed a reduction peak at − 885 V (scan rate of 0.1 V s^{-1}) [Fig. S5].

Voltammograms for reduction of the nitro group were also obtained at various scan rates for both compounds. I_{pc} was plotted against square root of scan rate according to Eq. 1 for both compounds (Fig. S6). Straight lines were obtained passing through the origin that clearly demonstrated the compounds undergo reduction in a diffusion-controlled pathway and that there was no adsorption on the electrode surface. Comparing the voltammogram of Onz with that of $[Cu_2(OAc)_4(Onz)_2]$, we found a two-fold increase in reduction peak current (I_{pc}) for the complex compared to Onz (Fig. S5) [17].

DNA binding studies

Under the experimental conditions, Onz shows a reduction peak at -900 mV while $[Cu_2(OAc)_4(Onz)_2]$ shows a peak at -885 mV. In case of Onz, on increasing the concentration of c t DNA, the peak current gradually decreased (Fig. 4) while for $[Cu_2(OAc)_4(Onz)_2]$, the peak current gradually increased (Fig. S7). Based on the change in peak current (ΔI) for Onz and the complex binding constants were evaluated considering the equilibrium in Eq. 2.

$$L + DNA = L - DNA; \quad K_d = \frac{[L][DNA]}{[L - DNA]} \qquad (2)$$

In case of Onz, a decrease in peak current during titration with DNA is suggestive of the fact that the nitro group of Onz immediately upon formation of the nitro radical anion interacts with DNA resulting in structural changes that progressively make it difficult for $-NO_2$ reduction electrochemically. This happens because as Onz molecules start interacting with DNA there occurs changes in the orientation of the nitro group of bound molecules preventing reduction. Hence this attribute of unbound molecules making their nitro groups available for reduction i. e. being able to interact with electrons at the electrode surface was used to measure the amount of Onz interacting with c t DNA. However, the situation is exactly the reverse in case of the

complex. Here upon adding DNA, the peak increases implying the nitro group of the bound form of the complex not only remains electrochemically active but is definitely more suited to reduction at the electrode surface. If this was not the case then during titration for a fixed concentration of the complex there is no reason why successive currents (I_{pc}) should increase with addition of DNA. This increase in peak current could then be used as a measure of the extent of interaction between $[Cu_2(OAc)_4(Onz)_2]$ and c t DNA. Hence, at any point of the titration of the complex, the cathodic peak current corresponds to contributions both from free and bound forms. Thus, ΔI for the complex corresponds to $(m'c_b^i - mc_f^i)$ where c_b^i refers to the concentration of the bound form of $[Cu_2(OAc)_4(Onz)_2]$, c_f^i being its corresponding concentration in the absence of DNA.[32] m is a constant equal to $0.4463\ (F^3/RT)^{1/2}\ n^{3/2}\ A_0\ D_{[Cu2(OAc)4(onz)2]}^{1/2}\ v^{1/2}$ for the free form of $[Cu_2(OAc)_4(Onz)_2]$ while m' is the same constant for the bound form of $[Cu_2(OAc)_4(Onz)_2]$.[32]

Equation SE 1 is a linear plot of the reciprocal of ΔI with the reciprocal of $(C_D - C_0)$ whose slope provides an estimate of the dissociation constant $K_d = (1/K_{app})$ while the intercept yields $1/\Delta I_{max}$ (Fig. S8). K_{app} denotes the apparent binding constant for the interaction (Table 2). The value of ΔI_{max} was used to find the ratio $\Delta I/\Delta I_{max}$ which was then plotted against concentration of added c t DNA. This was done for both compounds and the plot was fitted according to the non-linear square fit analysis, [Eqs. SE 2 and SE 3] (Fig. 5). K_{app} obtained from double reciprocal and non-linear fits were compared (Table 2). Site size of interaction (n_b) was determined with the help of the mole ratio plot (Fig. S9) where $\Delta I/\Delta I_{max}$ was plotted against ratio of the concentration of DNA to that of the compounds. n_b denotes the number of nucleotide bases bound to a molecule of each compound. Multiplying K_{app} with n_b the overall binding constant (K^*) was obtained.[17] The titrimetric data was also fitted to the Scatchard equation (Eq. SE 4, Fig. 6) and overall binding constant and site size of interaction was evaluated for both compounds (Table 2).

Binding parameters were more or less similar for both compounds. Hence, in this case, the DNA interaction study does not attest to complex formation being regarded as an improvement in the direction of biological activity.

Interaction of Onz and $[Cu_2(OAc)_4(Onz)_2]$ with bacterial cells

Efficacy of the compounds was studied on two bacterial strains. Results suggest Onz and $[Cu_2(OAc)_4(Onz)_2]$ are almost comparable in their performance on *Staphylococcus aureus* (ATCC 29213) and *Escherechia coli* (ATCC 25922) as revealed by MIC assay. MIC values were found in the range 20.25 μM to 40.5 μM for both compounds (Table ST4, S I). Control experiments were done using free $Cu^{(II)}$ from copper$^{(II)}$ nitrate and copper$^{(II)}$ acetate, a $Cu^{(II)}$ complex of a non-toxic ligand EDTA, EDTA itself in the form of Na_2EDTA and a 1:1 mixture of Onz and Cu^{II} (taken as $Cu(OAc)_2.H_2O$). The control experiments showed free Cu(II) was not active against cells, registering a very high MIC value. Experiments carried out with the $Cu^{(II)}$ complex of EDTA did not show significant activity and was similar to that obtained with EDTA. The mixture of the 1:1 mixture of Onz and $Cu^{(II)}$ showed results exactly similar to that observed for Onz (Table ST4, S I). An earlier study with the dimeric $Cu^{(II)}$ complex of tnz revealed that the complex had a lower MIC value on the same bacterial cells than tnz.[17]

Conclusion

A Cu(II) complex of ornidazole was prepared and characterized. Using Onz and the complex we showed that the complex was able to drastically decrease the formation of the nitro-radical anion in an enzyme assay where hypoxanthine reduces the nitro group in the presence of Xanthine oxidase. DNA binding experiments with Onz and the complex revealed no improvement in binding in favor of the complex. However, efficacy of the complex remained unaltered towards

bacterial cells *Staphylococcus aureus* and *Escherechia coli*. Since formation of the nitro radical anion is responsible for antiparasitic - antibacterial activity as well as toxic side effect to the central nervous system it appears from this study even with decreased nitro radical anion the complexes are quite active. This study therefore suggests complex formation strikes the correct balance for the generation of nitro radical anion that is able to maintain efficacy on bacterial cells, leaving no excess for toxic side effects.

Experimental

Materials

Onz and copper(II) acetate [$Cu(OAc)_2.H_2O$] were purchased from Sigma-Aldrich, USA and E. Merck, India respectively. These were used without further purification for preparing the Cu^{II} complex of Onz. Hypoxanthine was obtained from Sisco Research Laboratories, India. Xanthine oxidase (XOD) isolated from cow milk was obtained from Sigma Aldrich as a suspension in ammonium sulphate solution. Calf thymus DNA was purchased from Sisco Research Laboratories and dissolved in triple distilled water. Concentration of c t DNA in terms of nucleotide was determined considering the molar extinction coefficient at 260 nm to be 6600 mol^{-1} dm^3 cm^{-1}. Aqueous solution of Tris buffer (Spectrochem Pvt. Ltd., India) having pH ~7.4 and NaCl (AR, Merck, Germany) was used to maintain physiological conditions in DNA binding experiments. Stock solutions of Onz and [$Cu_2(OAc)_4(Onz)_2$] were prepared in ethanol. All experimental solutions were prepared in triple distilled water.

Bacterial strains: Staphylococcus aureus (ATCC 29213) and Escherichia coli (ATCC 25922) were used in this study.[33–35] The strains were stored at −70 °C in 15% (vol/vol) glycerol until

subcultured onto respective media. Bovine heart infusion media (High Media Laboratories, India) was used for culturing bacterial cells.

Methods

Preparation of [Cu_2 $(OAc)_4(Onz)_2$]

The complex $[Cu_2(OAc)_4(onz)_2]$ was prepared by methods described earlier.[15-17] A solution of ornidazole (0.22 g, 1.00 mmol) in hot methanol (25 ml) was added to a solution of $Cu(OAc)_2.H_2O$ (0.2g, 1.00 mmol) in hot methanol (25 ml). The mixture was heated under reflux at a temperature of ~ 60^oC for 6 hours. Green crystals were obtained after a week by slow evaporation of the solvent. Yield: 78 %. Anal. Calc. (%) for $[Cu_2(OAc)_4(Onz)_2]$ i.e. C_{22} H_{30} Cu_2 N_6 O_{14} Cl_2: C, 33.00; H, 3.75; N, 10.50. Found: C, 33.07; H, 3.72; N, 10.56. Cu(II) present in the complex was estimated using standard procedure (Found: 15.76 % Anal. Calc.: 15.875 %).[36]

Crystallographic Data Collection and Refinement

Single crystals of the complex, having suitable dimensions, were used for data collection using a 'Bruker SMART APEX II' diffractometer equipped with graphite-monochromated Mo-Kα radiation (λ = 0.71073 Å) at 298 K. The molecular structures were solved using the SHELX-97 package.[37] Non-hydrogen atoms were refined with anisotropic thermal parameters. The hydrogen atom attached to oxygen was located by difference Fourier maps and was kept at fixed position. All other hydrogen atoms were placed in their geometrically idealized positions and constrained to ride on their parent atoms. Multi-scan empirical absorption corrections were applied to the data using the program SADABS.[38] CCDC reference number is 1016461. The figures were prepared using DIAMOND[39] and ORTEP.[40]

Physical measurements

FTIR data of solid samples as KBr pellets were obtained in the range 4000-400 cm^{-1} using a Perkin Elmer RX-I spectrophotometer. UV-Vis spectra for ornidazole and $[Cu_2(OAc)_4(Onz)_2]$ in methanol were recorded on a JASCO V-630 spectrophotometer, JASCO, Japan. Magnetic susceptibility measurements of powdered samples at room temperature (298 K) were recorded by Gouy method using Magway MSB MK1, Sherwood Scientific Ltd. EPR was recorded on JEOL JES-FA 200 ESR Spectrophotometer. Mass spectrum was recorded on Micromass Q-Tof micro^{TM}, Waters Corporation.

Enzyme assay

The method for enzyme assay, previously reported in the literature, uses xanthine oxidase (XOD) as a model nitro-reductase.[24] Hypoxanthine was the reducing substrate while Onz and $[Cu_2(OAc)_4(Onz)_2]$ were electron acceptors. The XOD suspension (225 µL) was diluted to 1.5 mL with 0.025 M phosphate buffer (pH 7.4) in a quartz cuvette sealed with a rubber septum. Oxygen was purged of by the passage of a stream of argon through the solution. The enzyme (XOD) solution had a specific activity of 0.3 units/mg of protein and contained ~10 units in 1.5 mL. In another quartz cuvette, 1.0 mL hypoxanthine (0.01M) in 0.1 M phosphate buffer (~pH 7.4) was taken along with 125 µL of 1600 µM Onz or $[Cu_2(OAc)_4(Onz)_2]$, that was earlier dissolved in DMF. The volume was made up to 2.0 mL with phosphate buffer (0.1M). The cuvette was sealed with a rubber septum and oxygen was purged of by the passage of argon through the solution. To initiate the reaction, 500 µL of the deoxygenated enzyme solution maintained in another cuvette, was added with the help of a gas-tight syringe to the degassed solution containing hypoxanthine and test compounds. The final assay solution (2.5 mL) was 0.26 units/mL in XOD, 80 µM with regard to either Onz or $[Cu_2(OAc)_4(Onz)_2]$ and 4 mM in hypoxanthine. The cuvette was inverted to mix and monitored by UV-Vis spectroscopy against a

buffer-DMF blank. Spectrum of the solutions for the assay was taken every 5 minutes for 2 hours. The change in absorbance at 320 nm was noted for Onz and $[Cu_2(OAc)_4(Onz)_2]$.

Cyclic voltammetry of Onz and $[Cu_2(OAc)_4(Onz)_2]$

Cyclic voltammetry was carried out using Metrohm Autolab electrochemical analyzer. The conventional three- electrode system was used. A glassy carbon electrode of surface area 0.1256 cm^2 served as the working electrode, a platinum wire was the counter electrode while Ag/AgCl, satd.KCl was the reference electrode (0.199/V). Before an experiment, the solution was degassed for 30 min using high-purity argon. The temperature was maintained with the help of a circulating water bath. Results were analyzed according to the Randles-Sevcik equation [Eq. 1].[41,42] The electrochemical reduction of the nitro group in Onz and $[Cu_2(OAc)_4(Onz)_2]$ was used to understand interaction of the compounds with c t DNA.

$$i_{pc} = (2.69 \times 10^5).n^{3/2}. D_0^{1/2}.A.C. \nu^{1/2} \quad (1)$$

i_{pc} refers to current in amperes at the cathodic peak potential, n indicates total number of electrons involved in electrochemical reduction, D_0, diffusion coefficient of the species, A, area of electrode in cm^2, C, the concentration of the substance in moles/cm^3 and ν, scan rate in V s^{-1}.

DNA binding

Since the response of Onz and $[Cu_2(OAc)_4(Onz)_2]$ in the visible part of the electromagnetic spectrum was very weak, interaction of the compounds with DNA was not followed using absorption spectroscopy.[17] Again, although Onz and $[Cu_2(OAc)_4(Onz)_2]$ had an absorption at 318 nm, DNA interaction was not studied in this region since DNA itself absorbs at 260 nm and the tailing of its absorbance interferes with those of the compounds.[17,28] Interaction was not followed using fluorescence spectroscopy owing to lack of strong fluorescence in either compound. Hence,

we chose to study the interaction of Onz and $[Cu_2(OAc)_4(Onz)_2]$ using cyclic voltammetry monitoring the reduction of the nitro group.[17,28,43] Although compelled to use this technique it was actually a blessing in disguise since interaction of nitroimidazoles with DNA proceeds via formation of the nitro radical anion that can only be realized properly if the interaction is followed by cyclic voltammetry.[6,7,17,28,43] Change in response of the nitro radical anion was followed to understand interaction of the compounds with c t DNA.[7,17,43] Experiments were performed at a scan rate of 100 mV/sec. The change in current ΔI being a measure of the extent to which the compound interacts with the added c t DNA.[17,32,44] Change in ΔI was put in standard equations (supplementary section) yielding values for binding constants and site size of interaction.[17,32,44] 750 μL of 1000 μM Onz or $[Cu_2(OAc)_4(Onz)_2]$ along with 600 μL of 100 mM Tris buffer and 720 μL of 500 mM NaCl was taken in a cell for electrochemical analysis. Volume was made up to 3.0 mL using triple distilled water. The final working solution was 250 μM with respect to Onz or $[Cu_2(OAc)_4(Onz)_2]$, 20 mM in Tris buffer and 120 mM in NaCl. A glassy carbon electrode of surface area 0.1256 cm^2 served as the working electrode, a platinum wire as counter electrode while Ag/AgCl, satd. KCl was the reference electrode. The experimental solution was degassed for 30 min using high-purity argon prior to recording a voltammogram.

Biological assay on two bacterial strains

In vitro antimicrobial activity of the compounds with Staphylococcus aureus, ATCC 29213 (gram-positive bacteria) and Escherechia coli, ATCC 25922 (gram-negative bacteria) were studied by performing minimum inhibitory concentration (MIC) assay. This was determined in Mueller Hinton Broth (MHB, HiMedia Laboratories, India) by micro-dilution technique using a 96-well round-bottomed microtitre plate (Corning Incorporated, Corning, NY) according to Clinical Laboratory Standards Institute (CLSI 2006b, formerly NCCLS) guidelines with a final

inoculum of 2 × 10^5 CFU/mL. MIC was the lowest drug concentration preventing visible turbidity after 18 h of incubation at 37 °C.

Abbreviations used: Mnz: Metronidazole; Tnz: Tinidazole; Onz: Ornidazole; $[Cu_2(OAc)_4(Onz)_2]$: Cu^{II} complex of ornidazole; PFOR: pyruvate ferredoxin oxidoreductase; XOD: Xanthine oxidase; CV: cyclic voltammetry.

Acknowledgements

RCS expresses his gratitude to UGC, New Delhi for an SRF. DG wishes to thank UGC, New Delhi for a project fellowship. SD is grateful to the DST-FIST program operating at the Department of Chemistry, Jadavpur University for the X-ray diffractometer facility. Authors are grateful to Prof. Amitava De of Chemical Sciences Division, Saha Institute of Nuclear Physics, Kolkata and his research scholars Ankan Dutta Chowdhury and Nidhi Agnihotri for co-operation extended during cyclic voltammetry experiments. They are also grateful to Prof. Kalyan K. Mukherjea and his student Shiv Shankar Paul for help in recording EPR at the departmental facility. Authors are grateful to Dr. Arup Gayen of the Department of Chemistry, Jadavpur University for kindly providing Argon for enzyme assay experiments. SD is grateful to Dr. Shouvik Chattopadhyay and his research scholar Subrata Jana, Department of Chemistry, Jadavpur University for help in analyzing the X-ray diffraction data and for providing the IR data of the complex.

References:

1) S. L. Cudmore, K. L. Delgaty,S.F. Haywrad-McClelland, D.P Petrin, G.E. Garber, *Clin Microbiol Rev.,* 2004, **17**, 783-793.

2) D. I. Edwards, Comprehensive Medicinal Chemistry, Eds. C. Hansch, P. G Sammes, J. B. Taylor, Pergamon Press Oxford 1990, vol. 2, pp.725-751.

3) R. P. Mason, Free Radicals in Biology, Eds. W. A. Pryor, vol. V, Academic Press New York 1982, pp. 161-222.

4) S. Sood, A Kapil, *Ind. J Sex Transm Dis*., 2008, **29**, 7-14.

5) D. Petrin, K. Delgaty, R. Bhatt, G. Garber, *Clin Microbiol Rev*., 1998, **11**, 300-317.

6) D. I. Edwards, *Br J Vener Dis.,* 1980, **56**, 285–290.

7) D. I. Edwards, *Journal of Antimicrobial Chemotherapy.,* 1993, **31**, 9-20.

8) C. Walsh, Antibiotics: Actions, Origins, Resistance, Washington D.C.: American Society for Microbiology Press, 2003.

9) R. Chait, S. Shrestha, A. Shah, J-B. Michel, R. Kishony, *PLoS ONE* 2010, **5**, e15179. DOI: 10.1371/journal.pone.0015179.

10) D. Petrin, K. Delgaty, K. R. Bhatt, G. Garber, *Clin Microbiol Rev.,* 1998, **11**, 300-317.

11) D. N. R. Rao, R. P. Mason, *The Journal of Biological Chem*., 1987, **262**, 11731-11736.

12) V. N. Coleman, J. Halsey, R. S. Cox, V. K. Hirst, T. Blaschke, A. E. Howes, T. H. Wasserman, R. C. Urtasun, T. Pajak, S. Hancock, T. L. Philips, L. Noll, *Cancer Research*., 1987, **47**, 319-322.

13) J. A. Upcroft, L. A. Dunn, J. M. Wright, K. Benakli, P. Upcroft, P. Vanelle, *Antimicrob. Agents Chemother.*, 2006, **50**, 344-347.

14) A. W. Addison, T. Nageswara, J. Reedijk, J. van Rijn, G. C. Verchoor, *J. Chem. Soc., Dalton Trans.,* 1984, 1349-1356.

15) M. S. Nothenberg, S. B. Zyngier, A. M. Giesbrecht, M. T. P. Gambardella, R. H.A. Santos, E. Kimura, R. Najjar, *J. Braz. Chem. Soc.,* 1994, **5**, 23-29.

16) N. Galván-Tejada, S. Bernès, S. E. Castillo-Blum, H. Nöth, R. Vicente, N. Barba-Behrens, *J. Inorg. Biochem*., 2002, **91**, 339-348.

17) R. C. Santra, K. Sengupta, R. Dey, T. Shireen, P. Das, P. S. Guin, K. Mukhopadhyay, S. Das, *J. Coord. Chem.,* 2014, **67**, 265-285.

18) J. R. Wasson, C. Shyr, C. Trapp, *Inorg. Chem*., 1968, **7**, 469-473.

19) B. Kozlevčar, I. Leban, I. Turel, P. Šegedin, M. Petric, F. Pohleven, A. J. P. White, D. J. Williams, J. Sieler, *Polyhedron*, 1999, **18**, 755-762.

20) P. M. Selvakumar, E. Suresh, P. S. Subramanian, *Inorg. Chim. Acta*, 2008, **361**, 1503-1509.

21) R. Cejudo, G. Alzuet, J. Borrás, M Liu-González, F. Sanz-Ruiz, *Polyhedron*, 2002, **21**, 1057-1061.

22) R. W. Jotham, S. F. A. Kettle, J. A. Marks, *J. Chem. Soc., Dalton Trans*., 1972, 428-438.

23) S. Chavan, D. Srinivas, P. Ratnasamy, *J. Catal.*, 2000, **192**, 286-295.

24) K. E. Linder, Y-W. Chan, J. E. Cyr, M. F. Malley, D. P. Nowotnik, A. D. Nunn, *J. Med. Chem*., 1994, **37**, 9-17.

25) P. C. Mandal, D. K. Bardhan, S. N. Bhattacharyya, *Bull. Chem. Soc. Jpn*., 1990, **63**, 2975-2980.

26) K. D. Whitburn, M. Z. Hoffman, N. V. Brezniak, M. G. Simic, *Inorg. Chem*., 1986, **25**, 3037-3043.

27) T. Kagiya, H. Ide, S. Nishimoto, T. Wada, *Int. J. Radiat. Biol*., 1983, 44, 505-517.

28) P. C. Mandal, *J. Electroanal. Chem*., 2004, **570**, 55-61.

29) J. H. Tocher, D. I. Edwards, *Free Radical Res. Commun*., 1989, **6**, 39-45.

30) J. Carbajo, S. Bollo, L. J. Núñez-Vergara, P. A. Navarrete, J. A. Squella, *J. Electroanal. Chem*., 2000, **494**, 69-76.

31) J. H. Tocherz, D. I. Edwards, *Free Radical Res*., 1992, **16**, 19-25.

32) P. S. Guin, P. C. Mandal, S. Das, *ChemPlusChem*, 2012, **77**, 361–369.

33) A. Kohli, N. F. N. Smriti, K. Mukhopadhyay, A. Rattan, R. Prasad, *Antimicrob. Agents Chemother*., 2002, **46**, 1046-1052.

34) K. Mukhopadhyay, T. Prasad, P. Saini, T. J. Pucadyil, A. Chattopadhyay, R. Prasad. *Antimicrob. Agents Chemother*., 2004, **48**, 1778-1787.

35) Madhuri, T. Shireen, S. K. Venugopal, D. Ghosh, R. Gadepalli, B. Dhawan, K. Mukhopadhyay, *Peptides*, 2009, **30**, 1627-1635.

36) A. I. Vogel, A Text Book of Quantitative Inorganic Analysis, ELBS & Longman London 1961, pp. 902.

37) G. M. Sheldrick, SHELXS–97 and SHELXL–97, University of Göttingen, Germany, 1997.

38) G. M. Sheldrick, SADABS: Software for Empirical Absorption Correction, University of Gottingen, Institute fur Anorganische Chemieder Universitat, Gottingen, Germany, 1999-2003

39) H. Putz, K. Brandenburg, Diamond-Crystal and Molecular Structure Visualization; Crystal Impact Kreuzherrenstr 102, 53227 Bonn, Germany. http://www.crystalimpact.com/diamond

40) M.N. Burnett, C.K. Johnson, ORTEP-3: Oak Ridge Thermal Ellipsoid Plot Program for Crystal Structure Illustrations, Report ORNL-6895, Oak Ridge National Laboratory, Oak Ridge, TN, USA, 1996.

41) J. E. B. Randles, *Trans. Faraday Soc*., 1948, **44**, 327-338.

42) A. J. Bard, L. R. Faulkner, Electrochemical Methods Fundamental and Applications, John Wiley & Sons, Inc. New York, 2001.

43) X. Jiang, X. Lin, *Bioelectrochemistry,* 2006, **68**, 206-212.

44) P. S. Guin, S. Das, P. C. Mandal, *Int. J. Electrochem*., 2012, Article ID 183745, 10 pages, 2012. doi:10.1155/2012/183745.

Legends to Figures:

Fig. 1: ORTEP3 view of $[Cu_2(OAc)_4(Onz)_2]$ with 30% ellipsoid probability. Only relevant atoms are lebelled. Hydrogen atoms are not shown for clarity. Selected bond lengths (Å) and bond angles (°): Cu(1)–O(1) 1.978(2), Cu(1)–O(2) 1.961(1), Cu(1)–O(3) 1.948(1), Cu(1)–O(4) 1.981(1), Cu(1)–N(1) 2.185(3), O(1)-Cu(1)-O(4) 167.91(11), O(2)-Cu(1)-O(3) 167.55(9), O(1)-Cu(1)-N(1) 93.39(11), O(1)-Cu(1)-O(3) 91.42(6).

Fig. 2: UV-Vis spectra of Onz (A), $[Cu_2(OAc)_4(Onz)_2]$ and 1:1 mixture of Onz and $Cu(OAc)_2.H_2O$ (C) in the presence of xanthine oxidase and hypoxanthine in 5% DMF medium. Each spectrum was taken at 5 minutes interval.

Fig. 3: Comparison of the rate of reduction of Onz (■) and $[Cu_2(OAc)_4(Onz)_2]$ (•) and 1:1 mixture (▲) of Onz and $Cu(OAc)_2.H_2O$ under anaerobic conditions. (Initial

concentrations = 0.2 U/mL in XOD, 80 μM in Onz or $[Cu_2(OAc)_4(Onz)_2]$ or in the mixture, 4 mM in hypoxanthine, and 5% in DMF.

Fig. 4: Cyclic voltammograms obtained for Onz in the absence (1) and presence of different concentrations of c t DNA, 140.64μM (2), 279.43μM (3), 618.55μM (4), 946.87μM (5), 1783.26μM (6); [Onz] = 250 μM; [NaCl] = 120 mM; pH= 7.4; T = 25°C.

Fig. 5: Binding isotherm for Onz (A) and $[Cu_2(OAc)_4(Onz)_2]$ (B) interacting with c t DNA; the line is the fitted data corresponding to a non-linear fit that follows (Eqs. SE 2 and SE 3). [Onz] = $[Cu_2(OAc)_4(Onz)_2]$ = 250 μM, [NaCl] = 120 mM; pH= 7.4; T = 25°C.

Fig. 6: Titrations of Onz (A) and $[Cu_2(OAc)_4(Onz)_2]$ (B) with calf thymus DNA were fitted to Eq. SE 4 plotted as r/C_f vs. r; [Onz] = $[Cu_2(OAc)_4(Onz)_2]$ = 250 μM, [NaCl] = 120 mM; pH= 7.4; T = 25°C.

Tables

Table 1: Crystallographic and structural refinement parameters for $[Cu_2(OAc)_4(Onz)_2]$

Formula	$C_{22}H_{30}N_6O_{14}Cl_2Cu_2$
Formula Weight	800.52
Crystal Size (mm)	0.20 x 0.20 x 0.30
Temperature (K)	293
Crystal system	Monoclinic
Space group	$P2_1/c$
a(Å)	8.0418(7)
b(Å)	7.8054(6)
c(Å)	26.761(2)
β(deg)	*102.099(4)*
Z	*2*
d_{calc} (g cm-3)	*1.619*
μ(mm-1)	1.529
F(000)	816
Total Reflections	3761
Unique Reflections	3761
Observed data [I > 2 σ (I)]	1636
R1, wR2 (all data)	0.0134, 0.0469
R1, wR2 [I > 2 σ (I)]	0.0133, 0.0464
Largest diff. in peak and hole ($eÅ^{-3}$)	-0.28, 0.28

Table 2: Binding constants and site size of interactions

Compound	K_{app} (double reciprocal plot)	Kapp (non-linear plot)	Site size (mole ratio)	K^* (scatchard plot)	Site size (scatchard plot)
Onz	1.706×10^4	1.464×10^4	1.50	2.77×10^4	1.39
$[Cu_2(OAc)_4(Onz)_2]$	5.257×10^3	4.941×10^3	2.40	1.15×10^4	2.25

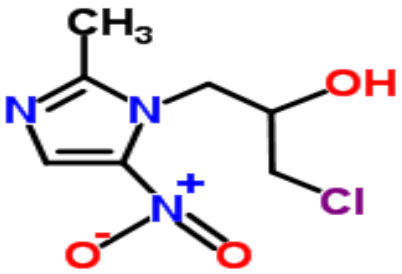

Onz

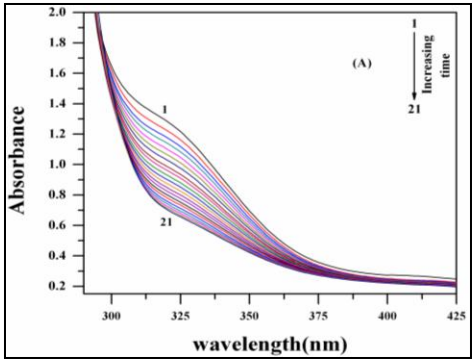

Substantial formation of $R\text{-}NO_2^{\cdot-}$ for Onz

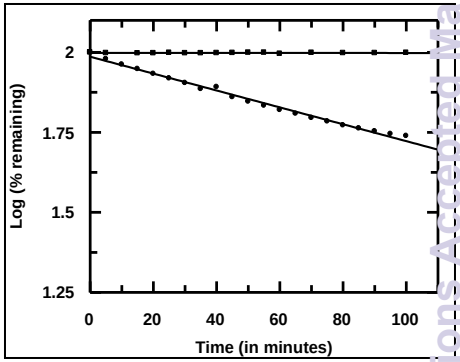

hypoxanthine

XOD

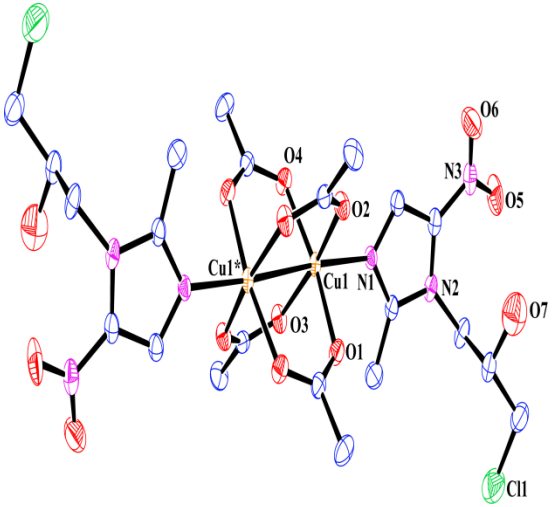

$[Cu_2(OAc)_4(Onz)_2]$

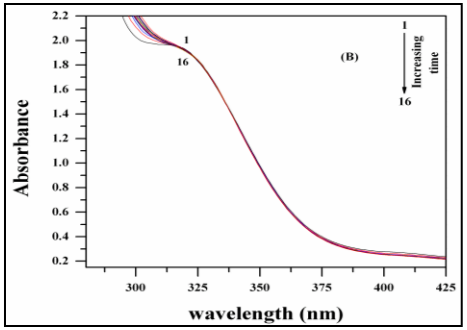

Decreased formation of $R\text{-}NO_2^{\cdot-}$ for complex

Fig. 1

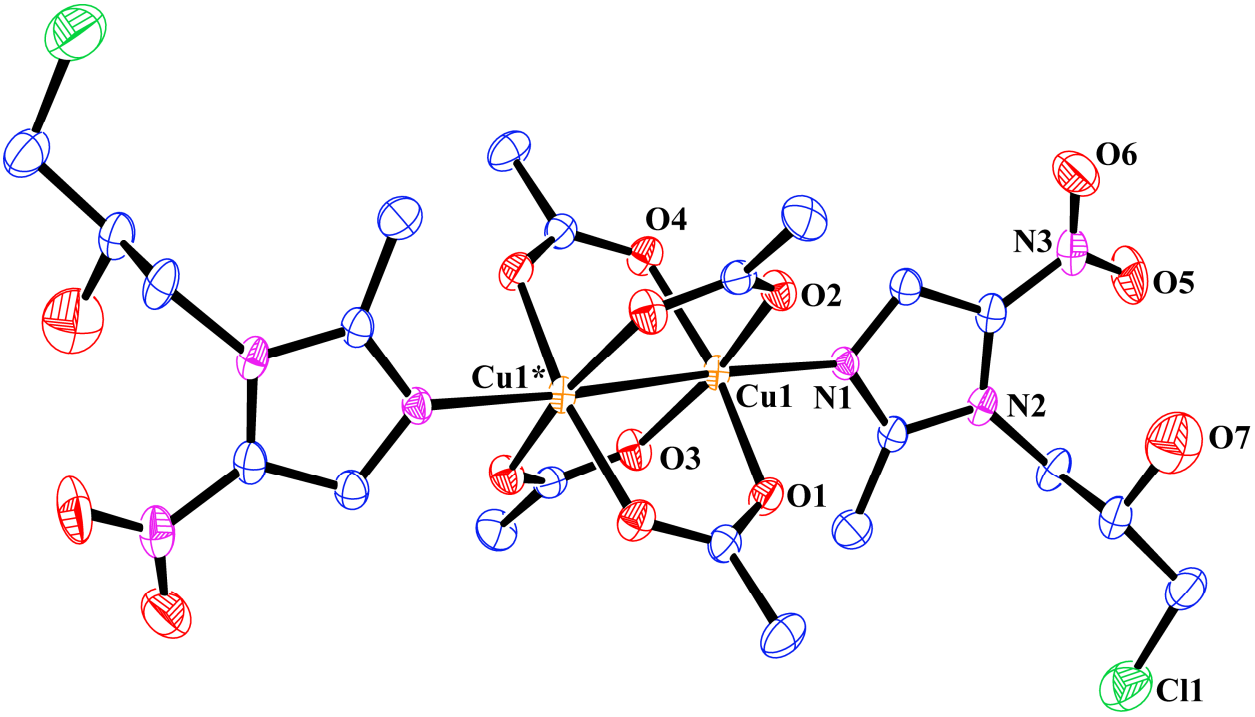

Fig. 2

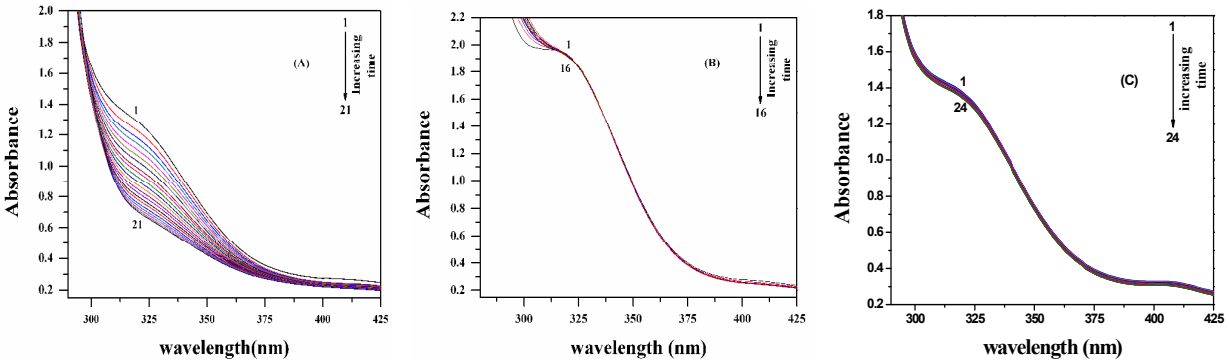

Fig. 3

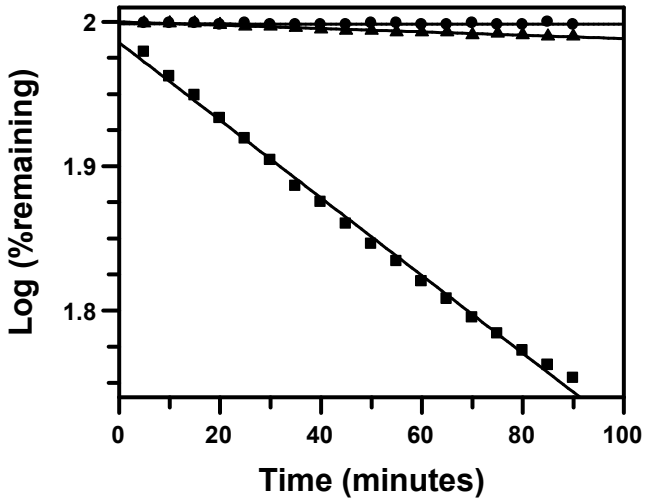

Fig. 4

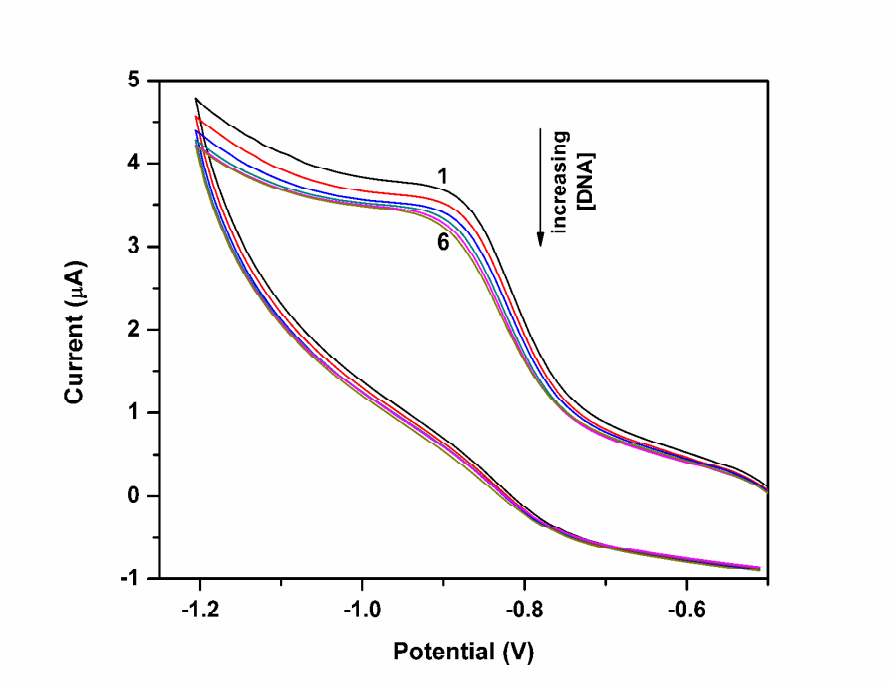

Fig. 5

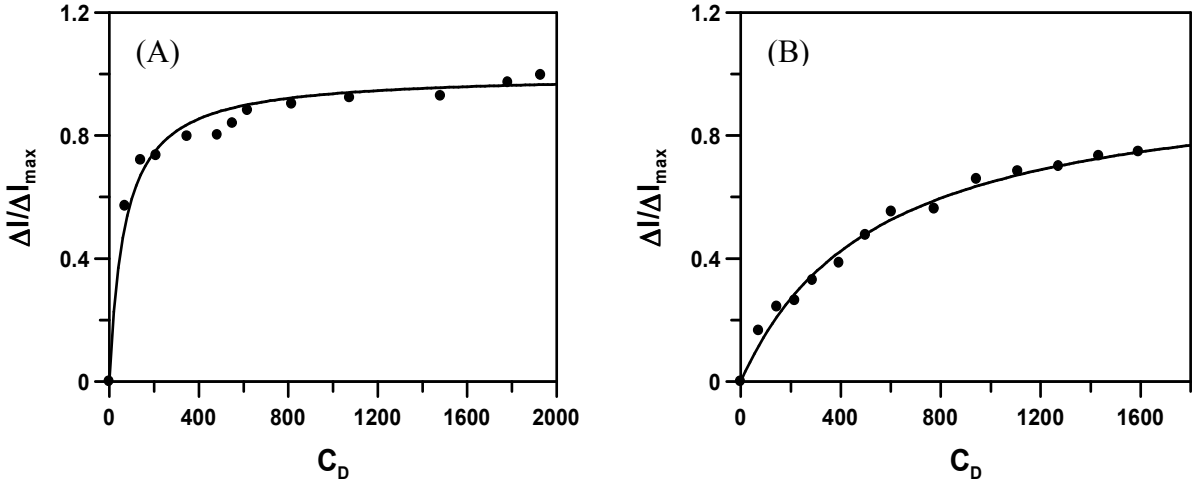

Fig. 6